

Unitary and analytic model of nucleon EM structure, the puzzle with JLab proton polarization data and new insight into proton charge distribution

C.Adamuščín¹, S.Dubnička¹, A.Z.Dubničková², P.Weisenpacher³

¹Institute of Physics, Slovak Academy of Sciences, Bratislava, Slovak Republic

²Department of Theoretical Physics, Comenius University, Bratislava, Slovak Republic

³Institute of Informatics, Slovak Academy of Sciences, Bratislava, Slovak Republic

June 25, 2018

Abstract

The Unitary and analytic model of nucleon electromagnetic structure, describing all existing nucleon form factor data, is briefly reviewed. Then in the framework of this model the problem of inconsistency of older proton electric form factor data in space-like region (obtained from $e^-p \rightarrow e^-p$ process by the Rosenbluth technique) with recent Jefferson Lab data on the ratio $G_{Ep}(t)/G_{Mp}(t)$ (measured in precise polarization $\vec{e}^-p \rightarrow e^-\vec{p}$ experiment) is suggested to be solved in favour of the latter data which, however, unlike older data cause an existence of the form factor zero, i.e. a diffraction minimum in $|G_{Ep}(t)|$ around $t = -Q^2 = -13\text{GeV}^2$. The new behaviour of $G_{Ep}(t)$ with the zero gives modified proton charge distribution with enlarged value of the mean square charge radius.

1 Introduction

The electromagnetic (EM) structure of nucleons is a manifestation of their quark structure in EM interactions, which can be completely described by four independent scalar functions of one variable ($t = -Q^2$, the squared four momentum transferred by the virtual photon) called EM form factors (FF's). The most suitable in extracting experimental information are Sachs electric $G_{EN}(t)$ and magnetic $G_{MN}(t)$ FF's, which in the Breit frame give the distribution of charge and magnetization within the nucleon, respectively.

Since the proton structure discovery in the middle of 50's of the last century until 2000 abundant and more or less accurate nucleon FF data in the space-like and time-like regions appeared and as result there are more than 500 experimental points with errors (see Figs 1,2) collected for qualified analyses.

Two problems appeared in relation to these so-called older nucleon FF data, in which proton electric and magnetic FF data in the space-like region are obtained (mainly in SLAC) from the measured differential cross sections of the elastic electron-proton scattering at different electron beam energies and subsequent utilization of the Rosenbluth technique to separate $G_{Ep}(t)$ and $G_{Mp}(t)$.

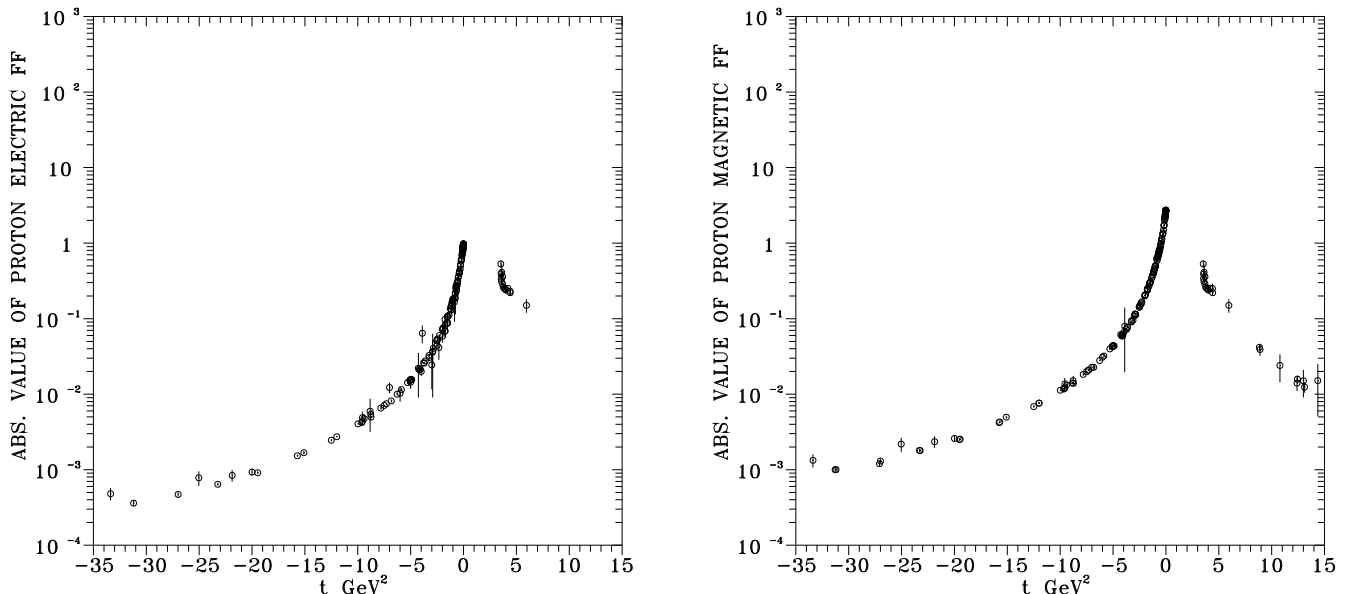


Figure 1: Experimental data on proton electric and magnetic form factors.

First, there was no well founded nucleon EM structure model (not even the dispersion theoretical approach [1-3]) to be successful in a description of these nucleon FF data in the space-like and time-like region simultaneously. In particular, the time-like magnetic neutron FF data caused problems.

Second, the recent Jefferson Lab data on $\mu_p G_{Ep}(Q^2)/G_{Mp}(Q^2)$, obtained [4,5] measuring simultaneously transverse

$$P_t = \frac{h}{I_0}(-2)\sqrt{\tau(1+\tau)}G_{Mp}G_{Ep}\tan(\theta/2) \quad (1)$$

and longitudinal

$$P_l = \frac{h(E+E')}{I_0 m_p}\sqrt{\tau(1+\tau)}G_{Mp}^2\tan^2(\theta/2) \quad (2)$$

components of the recoil proton's polarization in the electron scattering plane of the polarization transfer process $\vec{e}^- p \rightarrow e^- \vec{p}'$ (h is the electron beam helicity, I_0 is the unpolarized cross-section excluding σ_{Mott} and $\tau = Q^2/4m_p^2$) are in a rather strong disagreement with the data on $G_{Ep}(Q^2)$ obtained by Rosenbluth technique from differential cross-section on unpolarized electron scattering on protons.

The first problem was solved successfully in [6] and its solution will be briefly reviewed in the next Section. Section 3 will be devoted to the analysis of the second problem, utilizing unitary and analytic nucleon EM structure model from [6]. In the Section 4 consequences of the analysis of the Section 3 for the charge distribution within the proton are presented. The last Section contains a conclusion of the paper.

2 Unitary and analytic model of nucleon EM structure

In order to describe data in Figs. 1,2 we construct the model in the language of isoscalar and isovector parts of the Dirac and Pauli FF's to be related with Sachs electric and magnetic FF's by the expressions

$$\begin{aligned} G_{Ep}(t) &= [F_1^s(t) + F_1^v(t)] + \frac{t}{4m_p^2} [F_2^s(t) + F_2^v(t)] \\ G_{Mp}(t) &= [F_1^s(t) + F_1^v(t)] + [F_2^s(t) + F_2^v(t)] \\ G_{En}(t) &= [F_1^s(t) - F_1^v(t)] + \frac{t}{4m_p^2} [F_2^s(t) - F_2^v(t)] \end{aligned} \quad (3)$$

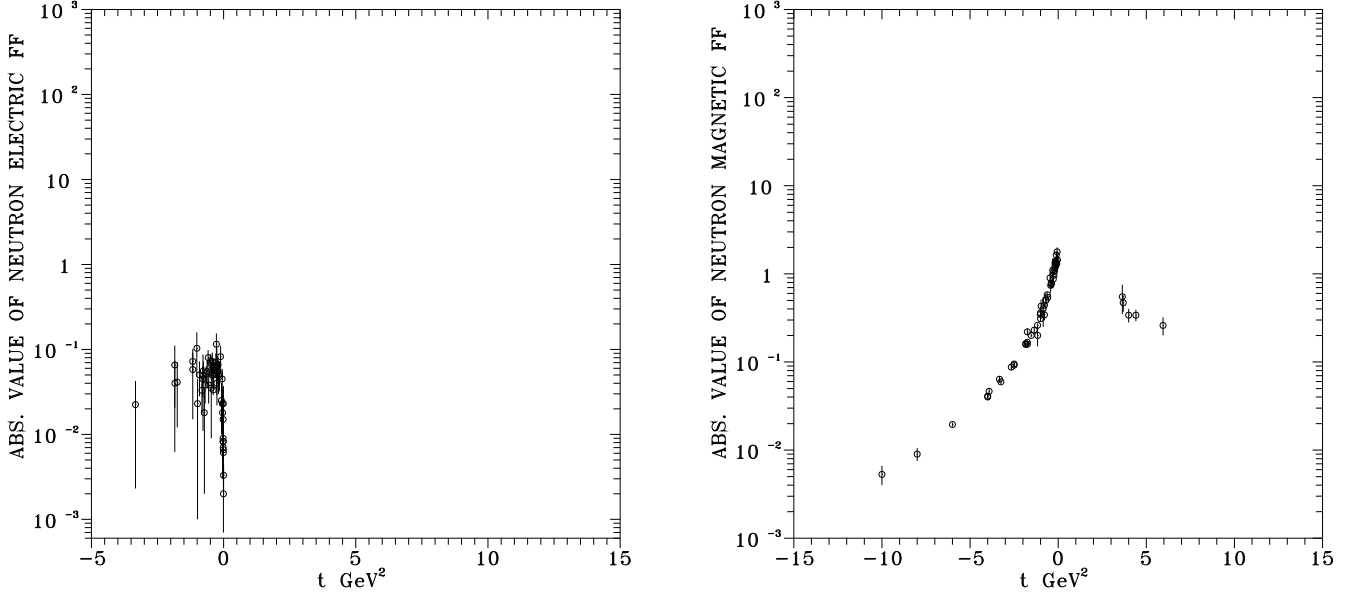


Figure 2: Experimental data on neutron electric and magnetic form factors.

$$G_{Mn}(t) = [F_1^s(t) - F_1^v(t)] + [F_2^s(t) - F_2^v(t)],$$

where then all known nucleon FF properties, like the experimental fact of a creation of unstable vector-meson resonances in the e^+e^- annihilation processes into hadrons, the hypothetical analytic properties (two-cut approximation) of nucleon EM FF's, by means of which just the contribution of continua are taken into account, the reality condition, the unitarity condition, normalizations, the asymptotic behaviour of FF's as predicted by quark model of hadrons are included. It has been manifested to be sufficient to saturate the isoscalar and isovector Dirac and Pauli FF's by 5 isoscalars ($\omega, \phi, \omega', \omega'', \phi'$) and 5 isovectors ($\rho, \rho', \rho'', \rho''', \rho''''$), first in the form of standard VMD parametrization, then utilizing the results of [7] it has been transformed to the form of the VMD parametrization to be automatically normalized with required asymptotic behaviour and finally, by using of the special nonlinear transformation and an introduction of the instability ($\Gamma_v \neq 0$) of the vector mesons under consideration, in the form of ten-resonance unitary and analytic model of nucleon EM structure as follows

$$\begin{aligned}
F_1^s[V(t)] = & \left(\frac{1 - V^2}{1 - V_N^2} \right)^4 \left\{ \frac{1}{2} H_{\omega''}(V) \cdot L_{\omega'}(V) + \left[H_{\omega''}(V) \cdot L_{\omega}(V) \cdot \frac{C_{\omega''}^{1s} - C_{\omega}^{1s}}{C_{\omega''}^{1s} - C_{\omega'}^{1s}} - \right. \right. \\
& - L_{\omega'}(V) \cdot L_{\omega}(V) \frac{C_{\omega'}^{1s} - C_{\omega}^{1s}}{C_{\omega''}^{1s} - C_{\omega'}^{1s}} - H_{\omega''}(V) \cdot L_{\omega'}(V) \left. \right] (f_{\omega NN}^{(1)} / f_{\omega}) + \\
& + \left[H_{\omega''}(V) \cdot L_{\phi}(V) \frac{C_{\omega''}^{1s} - C_{\phi}^{1s}}{C_{\omega''}^{1s} - C_{\omega'}^{1s}} - L_{\omega'}(V) \cdot L_{\phi}(V) \frac{C_{\omega'}^{1s} - C_{\phi}^{1s}}{C_{\omega''}^{1s} - C_{\omega'}^{1s}} - \right. \\
& - H_{\omega''}(V) \cdot L_{\omega'}(V) \left. \right] (f_{\phi NN}^{(1)} / f_{\phi}) - \left[H_{\phi'}(V) \cdot H_{\omega''}(V) \frac{C_{\phi'}^{1s} - C_{\omega''}^{1s}}{C_{\omega''}^{1s} - C_{\omega'}^{1s}} - \right. \\
& \left. - H_{\phi'}(V) \cdot L_{\omega'}(V) \frac{C_{\phi'}^{1s} - C_{\omega'}^{1s}}{C_{\omega''}^{1s} - C_{\omega'}^{1s}} + H_{\omega''}(V) \cdot L_{\omega'}(V) \right] (f_{\phi' NN}^{(1)} / f_{\phi'}) \left. \right\} \quad (4)
\end{aligned}$$

$$F_1^v[W(t)] = \left(\frac{1 - W^2}{1 - W_N^2} \right)^4 \left\{ \frac{1}{2} L_{\rho''}(W) \cdot L_{\rho'}(W) + \left[L_{\rho''}(W) \cdot L_{\rho}(W) \frac{C_{\rho''}^{1v} - C_{\rho}^{1v}}{C_{\rho''}^{1v} - C_{\rho'}^{1v}} - \right. \right.$$

$$\begin{aligned}
& - L_{\rho'}(W) \cdot L_{\rho}(W) \frac{C_{\varrho}'^{1v} - C_{\varrho}^{1v}}{C_{\varrho}''^{1v} - C_{\varrho}'^{1v}} - L_{\rho''}(W) \cdot L_{\rho'}(W) \Big] (f_{\varrho NN}^{(1)} / f_{\varrho}) + \\
& + \left[H_{\rho'''}(W) \cdot L_{\rho'}(W) \frac{C_{\varrho}'''^{1v} - C_{\varrho}'^{1v}}{C_{\varrho}''^{1v} - C_{\varrho}'^{1v}} - H_{\rho''}(W) \cdot L_{\rho''}(W) \frac{C_{\varrho}'''^{1v} - C_{\varrho}''^{1v}}{C_{\varrho}'^{1v} - C_{\varrho}^{1v}} - \right. \\
& - L_{\rho''}(W) \cdot L_{\rho'}(W) \Big] (f_{\varrho''' NN}^{(1)} / f_{\varrho'''}) - \left[H_{\rho'''}(W) \cdot L_{\rho''}(W) \frac{C_{\varrho}'''^{1v} - C_{\varrho}''^{1v}}{C_{\varrho}''^{1v} - C_{\varrho}'^{1v}} \right. \\
& \left. - H_{\rho'''}(W) \cdot L_{\rho'}(W) \frac{C_{\varrho}'''^{1v} - C_{\varrho}'^{1v}}{C_{\varrho}''^{1v} - C_{\varrho}'^{1v}} + L_{\rho''}(W) \cdot L_{\rho'}(W) \Big] (f_{\varrho''' NN}^{(1)} / f_{\varrho''''}) \Big\}
\end{aligned} \tag{5}$$

$$\begin{aligned}
F_2^s[U(t)] &= \left(\frac{1 - U^2}{1 - U_N^2} \right)^6 \left\{ \frac{1}{2} (\mu_p + \mu_n) H_{\omega''}(U) \cdot L_{\omega'}(U) \cdot L_{\omega}(U) + \right. \\
& + \left[H_{\omega''}(U) \cdot L_{\phi}(U) \cdot L_{\omega}(U) \frac{C_{\omega}''^{2s} - C_{\phi}^{2s}}{C_{\omega}''^{2s} - C_{\omega}'^{2s}} \cdot \frac{C_{\phi}^{2s} - C_{\omega}^{2s}}{C_{\omega}'^{2s} - C_{\omega}^{2s}} + \right. \\
& + H_{\omega''}(U) \cdot L_{\omega'}(U) \cdot L_{\phi}(U) \frac{C_{\omega}''^{2s} - C_{\phi}^{2s}}{C_{\omega}''^{2s} - C_{\omega}'^{2s}} \cdot \frac{C_{\omega}'^{2s} - C_{\phi}^{2s}}{C_{\omega}'^{2s} - C_{\omega}^{2s}} - \\
& - L_{\omega'}(U) \cdot L_{\phi}(U) \cdot L_{\omega}(U) \frac{C_{\omega}'^{2s} - C_{\phi}^{2s}}{C_{\omega}''^{2s} - C_{\omega}'^{2s}} \cdot \frac{C_{\phi}^{2s} - C_{\omega}^{2s}}{C_{\omega}'^{2s} - C_{\omega}^{2s}} - \\
& \left. - H_{\omega''}(U) \cdot L_{\omega'}(U) \cdot L_{\omega}(U) \right] (f_{\phi NN}^{(2)} / f_{\phi}) + \\
& + \left[H_{\phi'}(U) \cdot H_{\omega''}(U) \cdot L_{\omega'}(U) \frac{C_{\phi}'^{2s} - C_{\omega}''^{2s}}{C_{\omega}''^{2s} - C_{\omega}'^{2s}} \cdot \frac{C_{\phi}'^{2s} - C_{\omega}'^{2s}}{C_{\omega}'^{2s} - C_{\omega}^{2s}} - \right. \\
& - H_{\phi'}(U) \cdot H_{\omega''}(U) \cdot L_{\omega}(U) \frac{C_{\phi}'^{2s} - C_{\omega}''^{2s}}{C_{\omega}''^{2s} - C_{\omega}'^{2s}} \cdot \frac{C_{\phi}'^{2s} - C_{\omega}^{2s}}{C_{\omega}'^{2s} - C_{\omega}^{2s}} + \\
& + H_{\phi'}(U) \cdot L_{\omega'}(U) \cdot L_{\omega}(U) \frac{C_{\phi}'^{2s} - C_{\omega}'^{2s}}{C_{\omega}''^{2s} - C_{\omega}'^{2s}} \cdot \frac{C_{\phi}'^{2s} - C_{\omega}^{2s}}{C_{\omega}''^{2s} - C_{\omega}^{2s}} - \\
& \left. - H_{\omega''}(U) \cdot L_{\omega'}(U) \cdot L_{\omega}(U) \right] (f_{\phi' NN}^{(2)} / f_{\phi'}) \Big\}
\end{aligned} \tag{6}$$

$$\begin{aligned}
F_2^v[X(t)] &= \left(\frac{1 - X^2}{1 - X_N^2} \right)^6 \left\{ \frac{1}{2} (\mu_p - \mu_n) L_{\rho''}(X) \cdot L_{\rho'}(X) \cdot L_{\rho}(X) + \right. \\
& + \left[H_{\rho'''}(X) \cdot L_{\rho'}(X) \cdot L_{\rho}(X) \frac{C_{\varrho}'''^{2v} - C_{\varrho}'^{2v}}{C_{\varrho}''^{2v} - C_{\varrho}'^{2v}} \cdot \frac{C_{\varrho}'''^{2v} - C_{\varrho}^{2v}}{C_{\varrho}''^{2v} - C_{\varrho}^{2v}} - \right. \\
& - H_{\rho'''}(X) \cdot L_{\rho''}(X) \cdot L_{\rho}(X) \frac{C_{\varrho}'''^{2v} - C_{\varrho}''^{2v}}{C_{\varrho}''^{2v} - C_{\varrho}'^{2v}} \cdot \frac{C_{\varrho}'''^{2v} - C_{\varrho}^{2v}}{C_{\varrho}'^{2v} - C_{\varrho}^{2v}} + \\
& + H_{\rho'''}(X) \cdot L_{\rho''}(X) \cdot L_{\rho'}(X) \frac{C_{\varrho}'''^{2v} - C_{\varrho}''^{2v}}{C_{\varrho}''^{2v} - C_{\varrho}^{2v}} \cdot \frac{C_{\varrho}'''^{2v} - C_{\varrho}'^{2v}}{C_{\varrho}'^{2v} - C_{\varrho}^{2v}} - \\
& - L_{\rho''}(X) \cdot L_{\rho'}(X) \cdot L_{\rho}(X) \Big] (f_{\varrho''' NN}^{(2)} / f_{\varrho'''}) + \\
& + \left[H_{\rho'''}(X) \cdot L_{\rho'}(X) \cdot L_{\rho}(X) \frac{C_{\varrho}'''^{2v} - C_{\varrho}'^{2v}}{C_{\varrho}''^{2v} - C_{\varrho}'^{2v}} \cdot \frac{C_{\varrho}'''^{2v} - C_{\varrho}^{2v}}{C_{\varrho}''^{2v} - C_{\varrho}^{2v}} - \right.
\end{aligned} \tag{7}$$

$$\begin{aligned}
& - H_{\rho''''}(X) \cdot L_{\rho''}(X) \cdot L_{\rho}(X) \frac{C_{\rho''''}^{2v} - C_{\rho''}^{2v}}{C_{\rho''}^{2v} - C_{\rho'}^{2v}} \cdot \frac{C_{\rho''''}^{2v} - C_{\rho}^{2v}}{C_{\rho'}^{2v} - C_{\rho}^{2v}} + \\
& + H_{\rho''''}(X) \cdot L_{\rho''}(X) \cdot L_{\rho'}(X) \frac{C_{\rho''''}^{2v} - C_{\rho''}^{2v}}{C_{\rho''}^{2v} - C_{\rho}^{2v}} \cdot \frac{C_{\rho''''}^{2v} - C_{\rho'}^{2v}}{C_{\rho'}^{2v} - C_{\rho}^{2v}} - \\
& - L_{\rho''}(X) \cdot L_{\rho'}(X) \cdot L_{\rho}(X) \left. \left(f_{\rho'''' NN}^{(2)} / f_{\rho''''} \right) \right\}
\end{aligned}$$

where

$$\begin{aligned}
L_r(V) &= \frac{(V_N - V_r)(V_N - V_r^*)(V_N - 1/V_r)(V_N - 1/V_r^*)}{(V - V_r)(V - V_r^*)(V - 1/V_r)(V - 1/V_r^*)}; \\
C_r^{1s} &= \frac{(V_N - V_r)(V_N - V_r^*)(V_N - 1/V_r)(V_N - 1/V_r^*)}{-(V - 1/V_r)(V - 1/V_r^*)}; \quad r = \omega, \phi, \omega', \\
H_l(V) &= \frac{(V_N - V_l)(V_N - V_l^*)(V_N + V_l)(V_N + V_l^*)}{(V - V_l)(V - V_l^*)(V + V_l)(V + V_l^*)}; \\
C_l^{1s} &= \frac{(V_N - V_l)(V_N - V_l^*)(V_N + V_l)(V_N + V_l^*)}{-(V_l - 1/V_l)(V_l^* - 1/V_l^*)}; \quad l = \omega'', \phi', \\
L_k(W) &= \frac{(W_N - W_k)(W_N - W_k^*)(W_N - 1/W_k)(W_N - 1/W_k^*)}{(W - W_k)(W - W_k^*)(W - 1/W_k)(W - 1/W_k^*)}; \\
C_k^{1v} &= \frac{(W_N - W_k)(W_N - W_k^*)(W_N - 1/W_k)(W_N - 1/W_k^*)}{-(W_k - 1/W_k)(W_k^* - 1/W_k^*)}; \quad k = \rho, \rho', \rho'', \\
H_n(W) &= \frac{(W_N - W_n)(W_N - W_n^*)(W_N + W_n)(W_N + W_n^*)}{(W - W_n)(W - W_n^*)(W + W_n)(W + W_n^*)}; \\
C_n^{1v} &= \frac{(W_N - W_n)(W_N - W_n^*)(W_N + W_n)(W_N + W_n^*)}{-(W_n - 1/W_n)(W_n^* - 1/W_n^*)}; \quad n = \rho''', \rho'''' \\
L_r(U) &= \frac{(U_N - U_r)(U_N - U_r^*)(U_N - 1/U_r)(U_N - 1/U_r^*)}{(U - U_r)(U - U_r^*)(U - 1/U_r)(U - 1/U_r^*)}; \\
C_r^{2s} &= \frac{(U_N - U_r)(U_N - U_r^*)(U_N - 1/U_r)(U_N - 1/U_r^*)}{-(U - 1/U_r)(U - 1/U_r^*)}; \quad r = \omega, \phi, \omega', \\
H_l(U) &= \frac{(U_N - U_l)(U_N - U_l^*)(U_N + U_l)(U_N + U_l^*)}{(U - U_l)(U - U_l^*)(U + U_l)(U + U_l^*)}; \\
C_l^{2s} &= \frac{(U_N - U_l)(U_N - U_l^*)(U_N + U_l)(U_N + U_l^*)}{-(U_l - 1/U_l)(U_l^* - 1/U_l^*)}; \quad l = \omega'', \phi', \\
L_k(X) &= \frac{(X_N - X_k)(X_N - X_k^*)(X_N - 1/X_k)(X_N - 1/X_k^*)}{(X - X_k)(X - X_k^*)(X - 1/X_k)(X - 1/X_k^*)}; \\
C_k^{2v} &= \frac{(X_N - X_k)(X_N - X_k^*)(X_N - 1/X_k)(X_N - 1/X_k^*)}{-(X_k - 1/X_k)(X_k^* - 1/X_k^*)}; \quad k = \rho, \rho', \rho'', \\
H_n(X) &= \frac{(X_N - X_n)(X_N - X_n^*)(X_N + X_n)(X_N + X_n^*)}{(X - X_n)(X - X_n^*)(X + X_n)(X + X_n^*)}; \\
C_n^{2v} &= \frac{(X_N - X_n)(X_N - X_n^*)(X_N + X_n)(X_N + X_n^*)}{-(X_n - 1/X_n)(X_n^* - 1/X_n^*)}; \quad n = \rho''', \rho''''
\end{aligned}$$

and $V(t)$ (similarly $W(t), U(t)$ and $X(t)$) takes the form

$$V(t) = i \frac{\sqrt{\left(\frac{t_{in}^{1s}-t_0^s}{t_0^s}\right)^{1/2} + \left(\frac{t-t_0^s}{t_0^s}\right)^{1/2} - \sqrt{\left(\frac{t_{in}^{1s}-t_0^s}{t_0^s}\right)^{1/2} - \left(\frac{t-t_0^s}{t_0^s}\right)^{1/2}}}{\sqrt{\left(\frac{t_{in}^{1s}-t_0^s}{t_0^s}\right)^{1/2} + \left(\frac{t-t_0^s}{t_0^s}\right)^{1/2} + \sqrt{\left(\frac{t_{in}^{1s}-t_0^s}{t_0^s}\right)^{1/2} - \left(\frac{t-t_0^s}{t_0^s}\right)^{1/2}}} \quad (8)$$

with $t_0^s = 9m_\pi^2, t_0^v = 4m_\pi^2, t_{in}^{1v} = t_{in}^{2v} = 4m_N^2$ and t_{in}^{1s}, t_{in}^{2s} effective square root branch points, which however can not be fixed at two-nucleon threshold as in the isoscalar case there is a remarkable contribution of $K\bar{K}$ intermediate state in the unitarity condition.

Every FF, (4)-(7), represents always one analytic function for $-\infty < t < \infty$ to be defined on the four-sheeted Riemann surface, providing in such a way a very effective framework for a compatible superposition of complex conjugate vector-meson pole pairs on unphysical sheets and continua contributions in nucleon EM FF's.

If the parameters of $\rho, \omega, \phi, \rho', \omega', \phi', \rho'', \omega''$ are taken from Review of Particle Properties [8], the parameters of ρ''' from [9] and the parameters of ρ'''' are free we are left in $F_1^s[V(t)]$ with 4 free parameters, in $F_1^v[W(t)]$ with 3 free parameters, in $F_2^s[U(t)]$ with 3 free parameters and in $F_2^v[X(t)]$ with 4 free parameters. All of them are determined in comparison of the model with the collected 512 experimental points on the nucleon EM FF's in space-like and time-like region simultaneously and the fourth excited state of ρ -meson with the slightly lower mass $m_{\rho''''} = 1455 \pm 53 \text{ MeV}$ than in [10] and $\Gamma_{\rho''''} = 728 \pm 42 \text{ MeV}$ is determined. The quality of the achieved descriptions is graphically presented in Figs.3,4 by dashed lines.

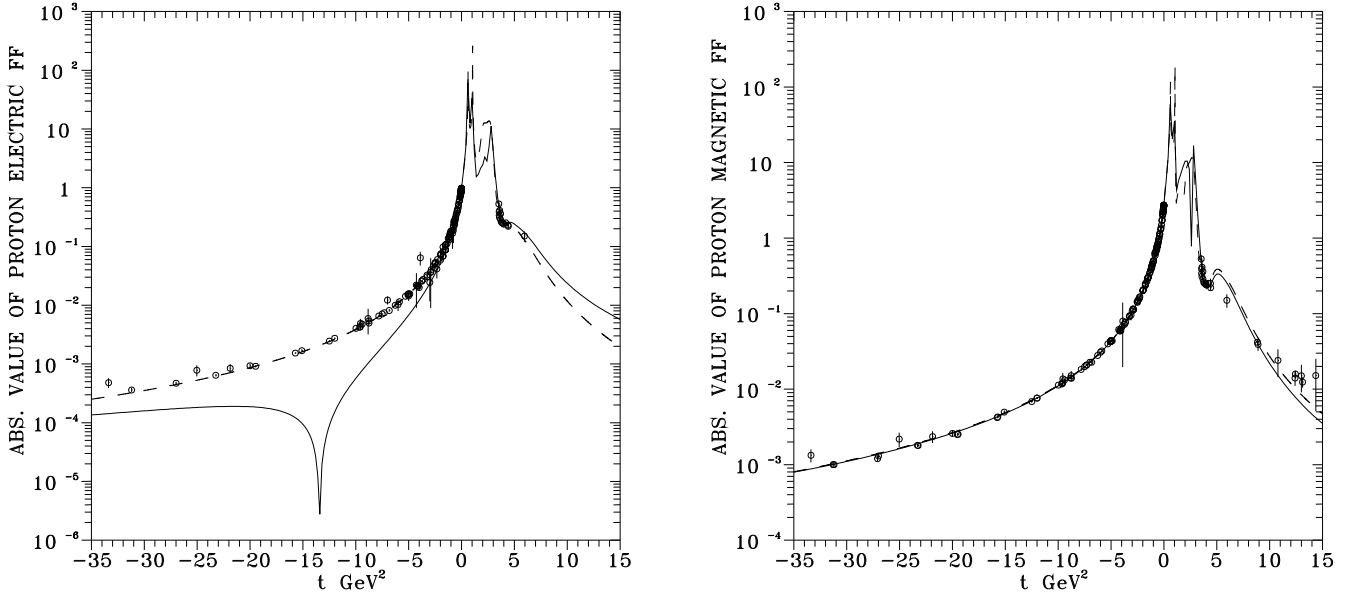


Figure 3: Theoretical behavior of proton electric and magnetic form factors.

3 JLab polarization data contradicting older SLAC $G_{Ep}(Q^2)$ behavior and the analysis of the puzzle

As we have mentioned at the Introduction there are new Jefferson Lab polarization data [4,5] on $\mu_p G_{Ep}(Q^2)/G_{Mp}(Q^2)$ for $0.49 \text{ GeV}^2 \leq Q^2 \leq 5.54 \text{ GeV}^2$ (see Fig.5) to be in rather strong disagreement

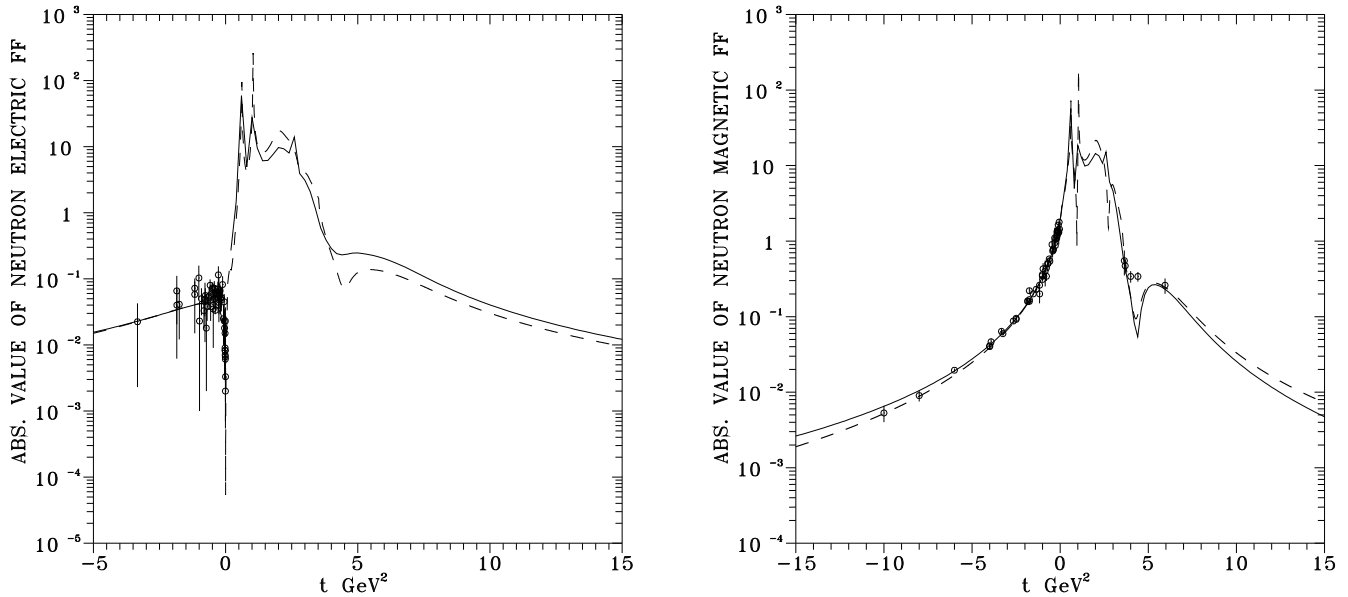


Figure 4: Theoretical behavior of neutron electric and magnetic form factors.

with the older separate data on $G_{Ep}(Q^2)$ and $G_{Mp}(Q^2)$ obtained in unpolarized elastic scattering of electrons on protons by the Rosenbluth technique. Really, whereas the older data on $G_{Ep}(Q^2)$ and $G_{Mp}(Q^2)$ follow (at least at the region of JLab data) a dipole behavior and their ratio with increased Q^2 is almost constant (see dotted line in Fig.5), the new precise JLab polarization data on $\mu_p G_{Ep}(Q^2)/G_{Mp}(Q^2)$ indicate, that $G_{Ep}(Q^2)$ behavior is somewhere between dipole and tripole one and to some extent it exhibits a violation of the pQCD prediction for the FF asymptotic behavior at the measured region.

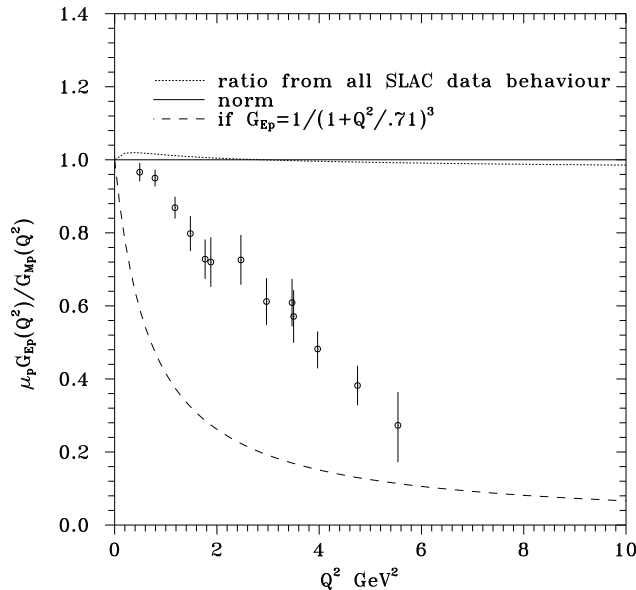


Figure 5: New JLab polarization data on the ratio $\mu_p G_{Ep}(t)/G_{Mp}(t)$

In order to solve this puzzle, one has to notice at the expression of the differential cross-section of the unpolarized elastic scattering of electrons on protons that due to the coefficient $-Q^2/4m_p^2$ in the front of $G_{Mp}^2(Q^2)$ the contribution of $G_{Ep}^2(Q^2)$ to the $d\sigma/d\Omega$ with increasing Q^2 is suppressed. For instance at $Q^2 = 3\text{GeV}^2$ the $G_{Ep}^2(Q^2)$ contributes with only 5% and with increased Q^2 it is even less. Then how it was possible by the Rosenbluth technique to draw out from $d\sigma/d\Omega$ so precise data on $G_{Ep}^2(Q^2)$

almost up to $Q^2 \approx 35\text{GeV}^2$? This question led us to the conjecture that may be data on $G_{Ep}(Q^2)$ in the space-like region extracted by Rosenbluth technique are unreliable and they should be ignored in the global analysis.

On the other hand, may be the very precise data on $\mu_p G_{Ep}(Q^2)/G_{Mp}(Q^2)$ obtained by measuring P_t and P_l of recoil proton's polarization in Jefferson Lab do not contradict predictions of pQCD (their steeper falling in comparison with the dipole behavior one could understand as finite momentum effect) and they are not in disagreement with all other known nucleon FF properties including also all other existing nucleon FF data.

In this spirit a discussion is carried out with only one aim to conserve as much as it is possible the one-photon exchange approximation validity in the electron-proton EM interactions, in the framework of which $d\sigma/d\Omega$ of the unpolarized elastic electron-proton scattering and also expressions for transverse P_t and longitudinal P_l components of the recoil proton's polarization in the electron scattering plane of the polarization transfer process $\vec{e}^- p \rightarrow e^- \vec{p}$ were derived.

Because recently it was suggested [11-13] that the two-photon corrections could resolve a large part of the discrepancy between the two abovementioned experimental techniques in the Born approximation. And if two-photon corrections play so important role in the elastic electron-proton scattering, what about an importance of two photon corrections in deep inelastic scattering (DIS), which could have unforeseen consequences.

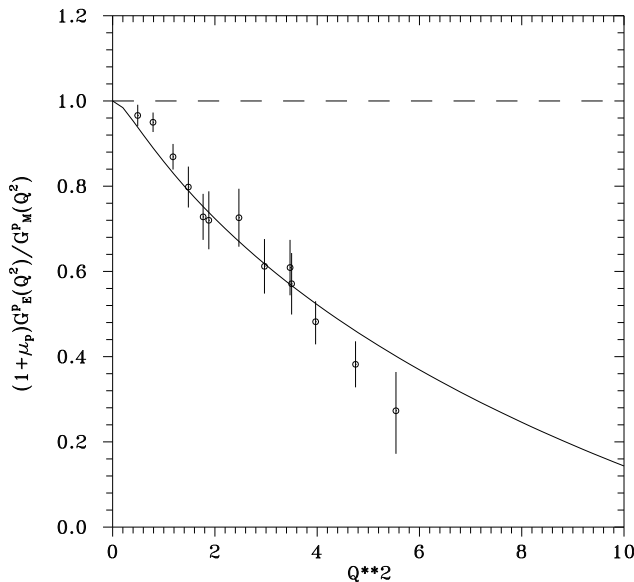


Figure 6: Description of the new JLab polarization data by ten-resonance unitary and analytic nucleon structure model

Therefore, in order to verify our above formulated conjecture, further we exclude all older space-like data on $G_{Ep}(t)$ obtained by Rosenbluth technique, then we substitute them only by Jefferson Lab polarization data on $\mu_p G_{Ep}(Q^2)/G_{Mp}(Q^2)$ and analyze the new data together with all electric proton time-like data and all space-like and time-like magnetic proton and electric and magnetic neutron data in the framework of the unitary and analytic nucleon EM structure model, formulated in Sec. 2 and comprising all nucleon FF properties, including also the asymptotic behavior of $G_{Ep}(t)$ predicted by pQCD.

As a result parameters of the model are changed very little, a perfect description of new JLab data is achieved (see Fig.6), almost nothing is changed in a description of $G_{Mp}(t)$, $G_{En}(t)$ and $G_{Mn}(t)$ in both, the space-like and time-like regions and $|G_{Ep}(t)|$ in the time-like region (see Figs.3,4). However, new JLab data on $\mu_p G_{Ep}(Q^2)/G_{Mp}(Q^2)$ strongly require the existence of a zero (see full-line in Fig.3a.),

i.e. the diffraction minimum in space-like region of $|G_{Ep}(t)|$ around $t = -Q^2 = -13\text{GeV}^2$, which could change the charge distribution behavior within proton.

4 Charge distribution within the proton

The proton charge distribution (assuming to be spherically symmetric) is an inverse Fourier transform of the proton electric FF

$$\rho_p(r) = \frac{1}{(2\pi)^3} \int e^{-iQr} G_{Ep}(Q^2) d^3Q \quad (9)$$

from where

$$\rho_p(r) = \frac{4\pi}{(2\pi)^3} \int_0^\infty G_{Ep}(Q^2) \frac{\sin(Qr)}{Qr} Q^2 dQ. \quad (10)$$

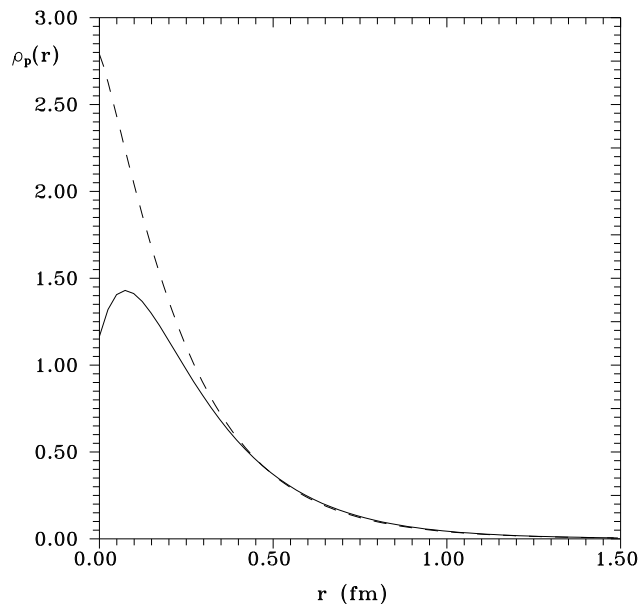


Figure 7: Charge distribution behavior within the proton

Substituting for the $G_{Ep}(Q^2)$ under the integral either the older behavior from Fig.3a given by dashed line, or the new behavior with the zero (see Fig.3a given by full line) following from the new JLab polarization data, one gets different charge distributions within the proton given in Fig.7 by dashed and full lines, respectively. That all leads also to different mean square proton radii. The old proton charge radius takes the value $\langle r_p^2 \rangle = 0.68\text{fm}^2$ and the new one $\langle r_p^2 \rangle = 0.72\text{fm}^2$.

5 Conclusions

On the basis of analysis of the new JLab polarization data on $\mu_p G_{Ep}(Q^2)/G_{Mp}(Q^2)$ in the framework of the ten-resonance unitary and analytic model we came to the conclusion, that they are consistent with all known nucleon FF properties and with all other existing FF data as well, besides the space-like data on $G_{Ep}(Q^2)$ obtained by Rosenbluth technique. They do not contradict the asymptotics predicted by pQCD, however they require an existence of zero around $t = -Q^2 = -13\text{GeV}^2$ and reveal a new knowledge on the proton charge distribution, leading to a larger mean square proton charge radius value.

References

- [1] P.Mergel, U.-G.Meissner and D.Drechsel, *Nucl. Phys. A* 596 367 1996
- [2] H.-W.Hammer,U.-G.Meissner and D.Drechsel, *Phys. Lett. B* 385 343 1996
- [3] S.Furuichi and D.Watanabe, *Nuovo Cimento A* 110 577 1997
- [4] M.K.Jones et al, *Phys. Rev. Lett.* 84 1398 2000
- [5] O.Gayon et al, *Phys. Rev. Lett.* 88 092301-1 2002
- [6] S.Dubnička, A.Z.Dubničková and P.Weisenpacher, *J. Phys. G* 29 405 2003
- [7] S.Dubnička, A.Z.Dubničková and P.Weisenpacher, *Eur. Phys. J. C* 32 381 2004
- [8] K.Hagivara et al, *Phys. Rev. D* 66 010001 2002
- [9] M.E.Biagini, S.Dubnička, E.Etim and P.Kolár, *Nuovo Cimento A* 104 363 1991
- [10] T.Frederico, H.-Ch.Pauli and Shan-Sui Zhan, *Phys. Rev. D* 66 116011 2002
- [11] P.A.M.Guichon and M.Vanderhaeghen, *Phys. Rev. Lett.* 91 142 304-1 2003
- [12] P.G.Blunder, W.Melnitchouk and J.A.Tjon, *Phys. Rev. Lett.* 91 142 304-1 2003
- [13] Y.-C.Chen et al, *Phys. Rev. Lett.* 93 122 301-1 2004